Near Neutrality of an Oxygen Molecule Adsorbed on a Pt(111) Surface

Liang Qi,[1] Xiaofeng Qian,[2] and Ju Li[1,*]

[1]*Department of Materials Science and Engineering, University of Pennsylvania, Philadelphia, Pennsylvania 19104, USA*
[2]*Department of Materials Science and Engineering, Massachusetts Institute of Technology, Cambridge, Massachusetts 02139, USA*

(Received 26 August 2007; revised manuscript received 31 March 2008; published 30 September 2008)

The charge state of paramagnetic or nonmagnetic O_2 adsorbed on a Pt(111) surface is analyzed using density functional theory. We find no significant charge transfer between Pt and the two adsorbed molecular precursors, suggesting these oxygen reduction reaction (ORR) intermediates are nearly neutral, and changes in magnetic moment come from self adjustment of O_2 spin-orbital occupations. Our findings support a greatly simplified model of electrocatalyzed ORR, and also point to more subtle pictures of adsorbates or impurities interacting with crystal than literal integer charge transfers.

DOI: 10.1103/PhysRevLett.101.146101 PACS numbers: 82.45.Jn, 82.65.+r

The adsorption of an O_2 molecule on a metal surface is an important process in surface physics and electrocatalysis [1–5]. Although the atomic geometries of O_2 adsorption can be accurately measured [1–4], the charge state of O_2^* ($*$ means adsorbed state or a free adsorption site) can only be inferred by indirect means such as vibrational frequency measurement. Under ultrahigh vacuum conditions, two bands of stretching mode of O_2^* on Pt (111) surface, 860–880 and 690–700 cm^{-1}, were identified and assigned as superoxide O_2^- and peroxide O_2^{2-} ion, respectively [1–3]. The charge assignment is crucial for understanding the mechanism of electrochemical oxygen reduction reaction (ORR), a complex multielectron transfer process. There has been a long debate on the existence of O_2^- as the intermediate in ORR [6]. Recently, Shao *et al.* measured oxygen vibrational spectra on Pt electrode in aqueous solution and suggested the formation of O_2^- as the first reaction step in electrocatalyzed ORR [5].

Ab initio modeling provides means to investigate the electronic structure of O_2^* quantitatively. Eichler and Hafner used density functional theory (DFT) calculation to study O_2 adsorption and identified superoxide O_2^- as a paramagnetic chemisorbed precursor at the bridge site of Pt(111) surface, and peroxide O_2^{2-} as a nonmagnetic precursor at the fcc hollow site, illustrated in Fig. 1(a) [7,8]. The formal charge assignments $^{1-}$ and $^{2-}$ were based on magnetic moments, vibrational frequencies and the *shape* of the charge difference density $\Delta\rho \equiv \rho[\mathrm{Pt(111)} + \mathrm{O_2}] - \rho[\mathrm{Pt(111)}] - \rho[\mathrm{O_2}]$ for these two O_2^* precursors. Since the vertical distance between O_2^* and surface is about 2 Å [7,8], these charge assignments would indicate large induced dipoles, defined as the difference in supercell total dipole before and after O_2 adsorption. However, this contradicts Hyman and Medlin's DFT study of oxygen molecule and atom adsorption on Pt(111) surface, where it was found that the induced electric dipole moments are very small (0.07 and 0.04 Åe for O_2^* and O^*, respectively) [9].

There is an urgent need to resolve this contradiction in order to understand the charge-transfer sequence of electrochemical ORR [10–12]. Recently, Nørskov *et al.* proposed a model to explain the origin of the ~0.4 volt cathode overpotential for ORR on Pt, as well as rank alloy catalytic activities, in significant agreement with experiments [12]. In this model, all the adsorbates such as O_2^*, OOH^*, O^*, and OH^* are assumed to be charge neutral, so the 4 electron transfers always occur concurrently with the 4 proton (hydronium) transfers from the electrolyte; i.e., all electron transfers are proton-coupled (PCET) [13]. Free-energy landscapes of the electrochemical ORR as a function of the electrode potential V were obtained, with the underlying assumption that the adsorption free energies of reaction intermediates are *unaffected* by V. This means very small electric dipoles induced by O_2^*, OOH^*, O^*, and OH^* in the surface normal direction, synonymous with the near-neutrality of these adsorbates, which needs to be justified in view of the conflicting reports [5,7–9].

To resolve this critical issue, we perform *ab initio* calculations of the adsorption of O_2 on Pt(111) surface and analyze the charge and spin densities quantitatively. We identify that there is no significant charge transfer between Pt surface and two chemisorbed precursors (paramagnetic and nonmagnetic). The change in magnetic moment is achieved by self-adjustments of occupations in two π^* antibonding orbitals in O_2^*.

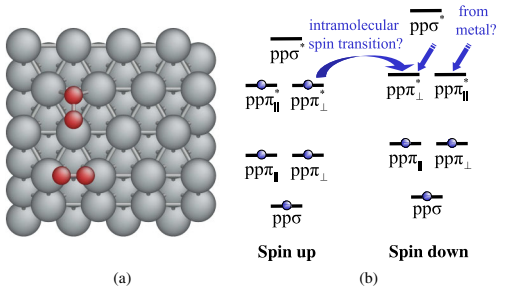

FIG. 1 (color online). (a) Configurations of two chemisorbed O_2 molecular precursors at the bridge site and fcc hollow site. (b) Molecular orbital energy diagram for O_2.

The calculations are performed using VASP [14,15]. We use projector augmented wave (PAW) potentials [16] with Perdew-Burke-Ernzerhof (PBE) exchange-correlation functional [17] in spin-polarized condition. The Pt(111) surface is modeled by a four-layer slab with a rectangular $\sqrt{3} \times 2$ unit cell of total 16 Pt atoms, separated by 12 Å thick vacuum layer. Only one oxygen molecule is adsorbed on one side of the slab: the molecule and Pt atoms at the top two layers are fully relaxed. Brillouin zone integrations are performed on a grid of $4 \times 4 \times 1$ $\vec{k}$ points, using first-order Methfessel-Paxton smearing of $\sigma = 0.2$ eV. The calculations are performed at equilibrium lattice constant of $a_0 = 3.977$ Å. Dipole corrections [18] of the electric potential and total energy are imposed to eliminate dipole-dipole interactions between image supercells. We have also checked the effects of larger supercell, symmetric adsorptions on both sides of the slab, larger vacuum region, higher density $\vec{k}$-points sampling in Brillouin zone and the usage of ultrasoft pseudopotentials with different functionals (LSD, PW91). In all cases, the changes in O_2^* charge state are not significant.

Table I shows the optimized geometry, E_{ad}, magnetic moment m, and stretching frequency ν of adsorbed O_2^*, most of which agree with Eichler and Hafner's results by ultrasoft pseudopotentials [7,8] and Shao's DFT calculations [5]. The magnetic moment density and total charge difference density are plotted and their shapes are seen to match Eichler and Hafner's plots [7,8]: for O_2^* at bridge site, its remaining magnetic moment density behaves like $\pi_{\parallel}^{\star}$ antibonding orbital; meanwhile, the *shape* of the charge difference density $\Delta\rho$ is similar to the $\pi_{\perp}^{\star}$ antibonding orbital [the molecular orbital energies of free O_2 are illustrate in Fig. 1(b), $\parallel$ and $\perp$ means parallel and perpendicular to the metal surface, respectively], so it was suggested that about one electron transferred from Pt to $\pi_{\perp}^{\star}$ spin-down orbital. On the other hand, for O_2^* at fcc hollow site, there is no magnetic moment left, and the shape of the charge difference density is like the sum of $\pi_{\perp}^{\star}$ and $\pi_{\parallel}^{\star}$, so it was suggested that about two electrons transferred from Pt to both $\pi_{\perp}^{\star}$ and $\pi_{\parallel}^{\star}$ spin-down orbitals. However, the induced dipole P_z, computed by direct charge integration in the supercell, is found by us to be small, only 0.06 and 0.07 eÅ for the bridge and fcc hollow site, respectively.

To analyze the charge state in a more fine-grained manner, we integrate the charge difference densities $\Delta\rho$ in x, y directions (parallel to the surface) and plot them with respect to z in Figs. 2(a) and 2(b) for paramagnetic and nonmagnetic case, respectively. It is seen that in both cases, the magnitude of $\Delta\rho$ is quite small, and inside the metal $\Delta\rho$ is more of the Friedel oscillation type than a net transfer. Only the metal surface charge density beyond the outermost Pt atom ($z > z_{Pt}$) shows appreciable net deficit, separated from the gain by O_2^* by a nodal structure at $z_{partition}$, indicated by the vertical dash lines in Figs. 2(a) and 2(b). We may thus define roughly the total electron transfer from Pt(111) to O_2^* molecule as

$$\Delta N \equiv \int_{z_{partition}}^{z_O+\Delta z} dz \iint dxdy \Delta\rho(x, y, z), \qquad (1)$$

where we take $z_{partition} = (z_{Pt} + z_O)/2$, z_{Pt} (z_O) being the highest (lower) z-coordinate of Pt(111) atoms (O_2^* molecule), respectively, and Δz is a distance from z_O to make sure that the charge density of O_2^* decays to essentially zero (here, we take $\Delta z = 5$ Å). Consistent with the dipole results, it is found that ΔN for both the paramagnetic bridge and nonmagnetic fcc hollow O_2^* are very small, just $0.07e$ and $0.09e$, respectively. To test the sensitivity on $z_{partition}$, with arbitrary choice of $z_{partition}$ between z_{Pt} and z_O, ΔN from charge difference integration is found to be always less than $0.13e$.

To reconcile the above with the observations of Eichler and Hafner [7,8], we find it instructive to also plot the *spin-charge difference*

$$\Delta\rho_\sigma \equiv \rho_\sigma[\mathrm{Pt(111)} + \mathrm{O_2}] - \rho_\sigma[\mathrm{Pt(111)}] - \rho_\sigma[\mathrm{O_2}] \quad (2)$$

in addition to the total charge difference, where σ denotes spin-up or -down state. The xy integral and isosurface of $\Delta\rho_\sigma$ are also shown in Fig. 2. We can see that changes in the spin charges are much larger in magnitude than change in the total charge, but there is a tremendous cancellation effect between $\Delta\rho_\uparrow$ and $\Delta\rho_\downarrow$. Using similar definition as Eqn. (1) for ΔN_σ, the spin-charge transfer for paramagnetic O_2^* at bridge site is found to be $\Delta N_\uparrow = -0.64e$ and $\Delta N_\downarrow = 0.71e$. Meanwhile, the isosurfaces of $\Delta\rho_\uparrow$ and $\Delta\rho_\downarrow$ [Fig. 2(a)] indicate that most of the spin-charge changes result from the decreased occupation of $\pi_{\perp}^{\star}$ spin-up orbital and increased occupation of $\pi_{\perp}^{\star}$ spin-down orbital. Such $\pi_{\perp\uparrow}^{\star} \rightarrow \pi_{\perp\downarrow}^{\star}$ transfer, illustrated in Fig. 1(b), causes no change in the total charge density, and thus would *not be detectable* in the total charge difference $\Delta\rho$ plot in spite of large activity.

For nonmagnetic O_2^* at fcc site, $\Delta N_\uparrow = -0.93e$ and $\Delta N_\downarrow = 1.02e$. The isosurfaces of $\Delta\rho_\uparrow$ and $\Delta\rho_\downarrow$ [Fig. 2(b)] show that both spin-charge differences have similar shape, which is a combination of $\pi_{\perp}^{\star}$ and $\pi_{\parallel}^{\star}$ orbitals, but are

TABLE I. DFT-PBE-PAW optimized O_2^* molecular precursors on Pt(111): the equilibrium bond length b, vertical distance z between O_2^* center and surface, adsorption energy E_{ad}, magnetic moment m, stretching frequency ν, and induced vertical electric dipole P_z.

	b[Å]	z[Å]	E_{ad}[eV]	$m[\mu_B]$	ν[cm^{-1}]	$\nu_{exp't}$[cm^{-1}]	$P_z[e$Å]
bridge	1.35	1.91	−0.65	0.93	913	870 [1], 875 [2]	0.06
fcc hollow	1.39	1.74	−0.53	0.00	826	710 [1], 700 [2]	0.07

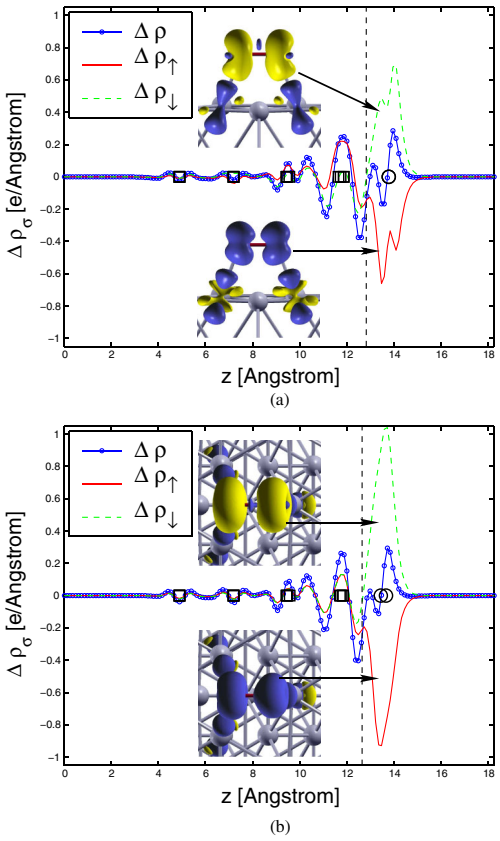

FIG. 2 (color online). Charge/spin-charge difference density $\Delta\rho/\Delta\rho_\sigma$ along the surface normal direction z for O_2^* at bridge (a) and fcc hollow (b) site on Pt (111) surface. Black squares/circles stand for the z-coordinates of Pt/oxygen atoms, and vertical dash lines stand for the middle position between the highest Pt and the lowest O atoms. The isosurfaces of $\Delta\rho_\uparrow$ and $\Delta\rho_\downarrow$ are plotted inside each subfigure using XCrySDen [23], where light and dark color means positive and negative change, respectively. The isovalues for all the isosurfaces are $\pm 0.04\ e\text{Å}^{-3}$.

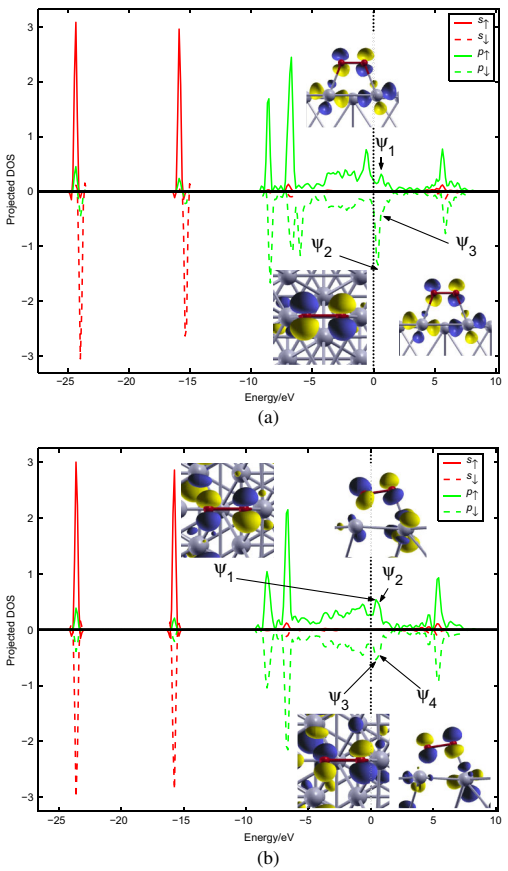

FIG. 3 (color online). Projected DOS of O_2^* at bridge (a) and fcc hollow (b) sites on Pt (111) surface. Fermi energy is zero and spin-down states are plotted as negative. Isosurfaces of the real part of Bloch eigenfunctions $\mathrm{Re}(\psi_{n\vec{k}})$ at $\vec{k} = [\frac{1}{8}\ \frac{1}{8}\ 0]$ of the first Brillouin zone are plotted for certain unoccupied peaks, as labeled in each subfigure. The absolute isovalues for all the isosurfaces are $\frac{1}{3}$ of the maximum absolute values of $\mathrm{Re}(\psi_{n\vec{k}})$ and light (dark) color means a positive (negative) value. For bridge-site case (a), the isosurfaces of ψ_1 ($n = 90$, $\epsilon = 0.54$ eV) and ψ_3 ($n = 89$, $\epsilon = 0.65$ eV) behave as spin-up and -down $\pi_\perp^\star$, respectively, while spin-down ψ_2 ($n = 90$, $\epsilon = 0.32$ eV) has the shape of $\pi_\parallel^\star$. For fcc-site case (b), isosurface of ψ_1/ψ_3 ($n = 89$, $\epsilon = 0.35$ eV) behaves as spin-up/down $\pi_\parallel^\star$, while ψ_2/ψ_4 ($n = 90$, $\epsilon = 0.52$ eV) is similar to spin-up/down $\pi_\perp^\star$.

opposite in sign. Hence, our new interpretation of O_2^* electronic structure is: when O_2 is adsorbed at bridge site of Pt(111) surface, about half electron transfers from $\pi_\perp^\star$ spin-up orbital to $\pi_\perp^\star$ spin-down orbital so that O_2^* is in a paramagnetic and almost neutral state; when O_2 is adsorbed at fcc hollow site, both spin-up $\pi_\perp^\star$ and spin-up $\pi_\parallel^\star$ give about half electron to their own spin-down orbitals so that O_2^* is nonmagnetic and also almost neutral. The transfer of electron occupation from metal to the molecule is only a "second-order" process relative to the "first-order" intramolecular spin transition.

Further analyses of the projected density of states (PDOS) of O_2^* and associated molecular orbital (MO) character of the Bloch eigenfunctions $\psi_{n\vec{k}}$ confirm our new interpretation. We plot the isosurface of the periodic part of $\mathrm{Re}(\psi_{n\vec{k}})$ corresponding to peaks in PDOS of O_2^*, as indicated by arrows in Fig. 3. For O_2^* at bridge site, beside the strong peak of unoccupied spin-down $\pi_\parallel^\star$ [labeled as ψ_2 in Fig. 3(a)], the spin-up or -down $\pi_\perp^\star$ [ψ_1 and ψ_3 in Fig. 3(a)] states are seen to be half occupied. At fcc site, there are also a large number of unoccupied states (spectral strength) just above the Fermi level, which can be clearly identified as having $\pi_\parallel^\star$ [labeled as ψ_1 and ψ_3 in Fig. 3(b)] and $\pi_\perp^\star$ [ψ_2 and ψ_4 in Fig. 3(b)] character. We also integrate the PDOS below the Fermi level for both O_2^* and isolated O_2 molecule with the same bond length as its adsorbed state. It is found that compared with isolated O_2, there are only slight changes in the occupied PDOS integral for adsorbed O_2^* (from $9.57e$ to $9.75e$ for O_2^* at bridge site, and $9.50e$ to $9.73e$ for O_2^* at fcc site), which also suggests no large electron transfer from Pt to oxygen.

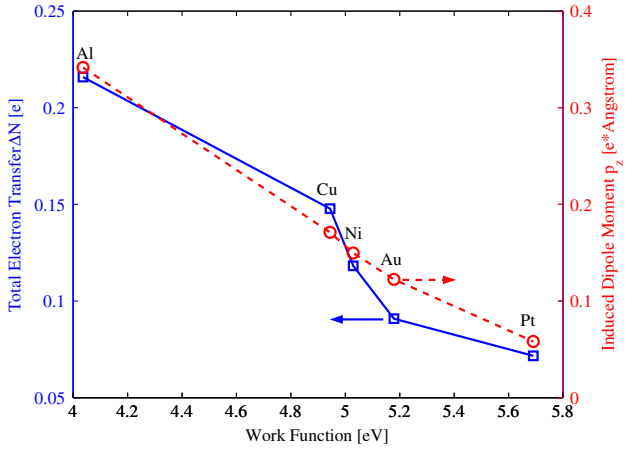

FIG. 4 (color online). Electron transfer ΔN and induced dipole P_z of O_2^* at bridge site versus (111) surface work function of different metals. The bond length of O_2^* and its distance to the top surface layer are fixed as the optimized values on Pt(111).

The next question is whether this small charge transfer during O_2 adsorption is just a special case for Pt(111) surface or a prevalent phenomenon on different metal surfaces. So we have used the same method to calculate the charge transfer and induced dipole moment when O_2 is adsorbed at the (111) surface bridge site of several other fcc metals with different work functions, as shown in Fig. 4. Although the tendencies of increasing charge transfer and induced dipole with decreasing work function are very clear, it is found that even for Al, which is very active and easy to lose electron, ΔN is only about $0.2e$. This result is consistent with a previous DFT calculation [19]. Under no circumstances can surface-adsorbed O_2^* be classified as a true integer anion [5]. Recently, Raebiger *et al.* found that transition metal impurities inside bulk ionic or semiconducting crystals maintain nearly constant local charge during redox [20]. Here, we demonstrate a similar phenomenon in molecular adsorptions on metal surfaces. Both challenge conventional notions of literal integer charge transfer between adsorbates or impurities and crystals.

In conclusion, *ab initio* calculations reveal that O_2^* adsorbed on a variety of metal surfaces possesses very little net charge and induced dipole. An intramolecular spin transition occurs when the molecule approaches the metal surface. So the adsorption energy and charge state of this important reaction intermediate are only weakly dependent on the electrode potential. The normal range of ORR cathode potential V is 0.6–1.0 volt with respect to the standard hydrogen electrode (SHE) and the potential of zero charge for Pt(111)-aqueous 0.1 M $HClO_4$ interface is about 0.2 volt versus SHE [21]. Suppose half of this interfacial potential variation physically localizes within the Helmholtz plane, usually 3 Å in thickness, the predicted variation in adsorption energy due to electrostatic effect will be $\sim$10 meV, smaller than k_BT. Additional calculations under strong external field (± 0.5 volt/Å) confirm that there are only small changes in both electron transfer and induced dipole moment, indicating small second-order (polarizability) effects [22]. The near-neutrality of reaction intermediates, and thus validated, enables one to greatly simplify the analysis and modeling of ORR electrocatalysis [12] for a wide range of electrode potentials.

We acknowledge support by Honda Research Institute USA, Inc. and thank Joshua Fujiwara for helpful discussions.

*liju@seas.upenn.edu

[1] J. L. Gland, B. A. Sexton, and G. B. Fisher, Surf. Sci. **95**, 587 (1980).
[2] H. Steininger, S. Lehwald, and H. Ibach, Surf. Sci. **123**, 1 (1982).
[3] D. A. Outka, J. Stohr, W. Jark, P. Stevens, J. Solomon, and R. J. Madix, Phys. Rev. B **35**, 4119 (1987).
[4] B. C. Stipe, M. A. Rezaei, W. Ho, S. Gao, M. Persson, and B. I. Lundqvist, Phys. Rev. Lett. **78**, 4410 (1997).
[5] M. H. Shao, P. Liu, and R. R. Adzic, J. Am. Chem. Soc. **128**, 7408 (2006).
[6] R. R. Adzic, in *Electrocatalysis*, edited by J. Lipkowski and P. N. Ross (Wiley, New York, 1998).
[7] A. Eichler and J. Hafner, Phys. Rev. Lett. **79**, 4481 (1997).
[8] A. Eichler, F. Mittendorfer, and J. Hafner, Phys. Rev. B **62**, 4744 (2000).
[9] M. P. Hyman and J. W. Medlin, J. Phys. Chem. B **109**, 6304 (2005).
[10] R. A. Sidik and A. B. Anderson, J. Electroanal. Chem. **528**, 69 (2002).
[11] Y. X. Wang and P. B. Balbuena, J. Phys. Chem. B **108**, 4376 (2004).
[12] J. K. Nørskov, J. Rossmeisl, A. Logadottir, L. Lindqvist, J. R. Kitchin, T. Bligaard, and H. Jonsson, J. Phys. Chem. B **108**, 17886 (2004).
[13] R. I. Cukier and D. G. Nocera, Annu. Rev. Phys. Chem. **49**, 337 (1998).
[14] G. Kresse and J. Hafner, Phys. Rev. B **47**, 558 (1993).
[15] G. Kresse and J. Furthmüller, Phys. Rev. B **54**, 11169 (1996).
[16] P. E. Blöchl, Phys. Rev. B **50**, 17953 (1994).
[17] J. P. Perdew, K. Burke, and M. Ernzerhof, Phys. Rev. Lett. **77**, 3865 (1996).
[18] G. Makov and M. C. Payne, Phys. Rev. B **51**, 4014 (1995).
[19] K. Honkala and K. Laasonen, Phys. Rev. Lett. **84**, 705 (2000).
[20] H. Raebiger, S. Lany, and A. Zunger, Nature (London) **453**, 763 (2008).
[21] M. Weaver, Langmuir **14**, 3932 (1998).
[22] L. Qi, X. Qian, and J. Li (to be published).
[23] A. Kokalj, Comput. Mater. Sci. **28**, 155 (2003).